Presented at 43rd European Photovoltaic Solar Energy Conference and Exhibition EUPVSEC
Rotterdam (Netherlands), 2026

Extension of Analytical Thermal Models to Assess Integrated Photovoltaics and Mobile Applications

Max Mittag, Alexander Protti, Christian Reichel, Dirk Holger Neuhaus
Fraunhofer Institute for Solar Energy Systems ISE
max.mittag@ise.fraunhofer.de

ABSTRACT: Analytical thermal models for photovoltaic (PV) modules are commonly based on one-dimensional heat-flow equations and are typically applied to free-standing modules with uniform environmental boundary conditions. This work extends an existing PV thermal model by enabling independent front- and rear-side parametrization of ambient temperature, wind speed, radiative surroundings, and ground properties. In addition, conductive heat transfer to a building wall and heat exchange with building interiors are introduced.
The extended model is integrated into a Cell-to-Module (CTM) loss-channel analysis framework and applied to a conventional glass-glass TOPCon module. Simulations are performed for free-standing PV, vehicle-integrated PV (VIPV), building-integrated PV (BIPV), building-attached PV (BAPV), and space PV applications.
The results demonstrate that application-specific boundary conditions strongly influence module temperature, dominant heat-transfer mechanisms, and power output. For the investigated module, efficiency decreases from 22.7% at standard test conditions to 19.5% under free-standing operating conditions, accompanied by a module temperature of 59.6 °C. VIPV benefits from strong convective cooling caused by vehicle motion, while BIPV achieves lower temperatures than BAPV due to heat conduction through the building wall. In space, radiative heat transfer is the only environmental heat-rejection mechanism, resulting in a simulated module temperature of 51.6 °C under 1367 W/m² AM0 irradiation.
The proposed model extensions enable thermal and electrical performance assessments of integrated PV applications.

I. INTRODUCTION

Several models for the analysis of the thermal behavior of photovoltaic (PV) modules have been published [1–7]. These models are very similar in their approach as they are all based on energy exchange between interfaces or through layers which is defined by a set of equations that can be solved assuming that an energy equilibrium must be present (Figure 1). The models are one-dimensional and calculate the temperature distribution along the PV module cross section. Spatial inhomogeneities are usually neglected. Direct heat transfer, convection, radiative heat exchange as well as heat sources and sinks attributed to specific layers or interfaces are considered.

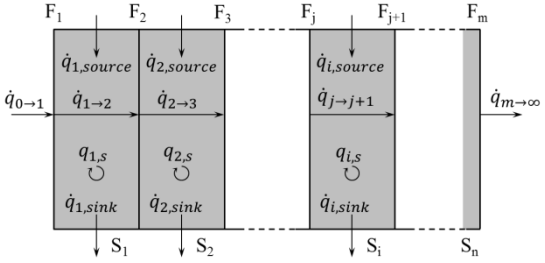

Figure 1: Thermal model with interfaces F, layers S and heat fluxes q, taken from [6]

At least a few of these models are also capable of dynamic calculations while the majority only analyses static conditions. The models are parametrized using layer or interface properties such as the layer thickness, the thermal conductivity, the interface emissivity or similar parameters. Another crucial input are the environmental conditions that are left constant when solving the set of equations of the thermal model.

A common application of this kind of model is the integration into a multi-physics modelling environment where optical losses in layers (that act as heat sources) and electrical models of the solar cells (where power generation acts as a heat sink) are combined with the thermal modelling. This enables the assessment of PV module technologies based on the module layer stack and the environmental conditions.

Integration of photovoltaic (PV) modules into other applications outside of commercial power plants is a megatrend that leads to many changes in module structure and design (i.e. materials, layout, process technologies). Methods are required that allow for a simulation-based assessment of these changes. The widely used CTM-analysis provides such method [3,8–13], but extensions are required to allow us to consider the specifics of each application.

We present an extension of the models based on new definitions of the applications environment and minor changes of the model itself. The changes and additions presented allow for a major extension of the capabilities of this group of analytical thermal models, namely the analysis of

a) Vehicle Integrated PV (VIPV),
b) Building Integrated PV (BIPV),
c) Building Attached PV (BAPV), and
d) Applications in space (SpacePV).

Also, the previously presented model [6] is extended, which improves flexibility for the analysis of free-standing PV modules.

Within this work we describe the changes to the thermal model and present results from analyses of the different application types.

We show that the application scenarios (or the prevalent boundary conditions for the thermal model in each application) have a significant impact on the module temperature, the heat exchange mechanisms as well as the module power output.

The presented changes and additions are effective and allow for a major extension of the capabilities of this group of analytical thermal models and the application to integrated photovoltaics.

II. METHODOLOGY

The existing model [6] is extended by introducing separate environmental conditions for the module front and rear side. Previously, the conditions were assumed to be uniform. Now, separate parametrization of the ground and sky in front and the back of the module is considered (Figure 2). This simple change allows the calculation of integrated and/or mobile PV applications.

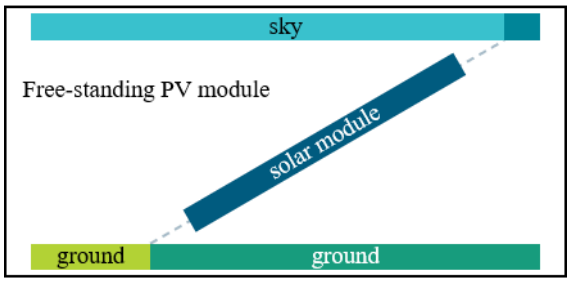

Figure 2: Schematic depiction of a free-standing PV module where the ground and the sky in the front and rear of the module are assumed to have different properties which are indicated by the respective color.

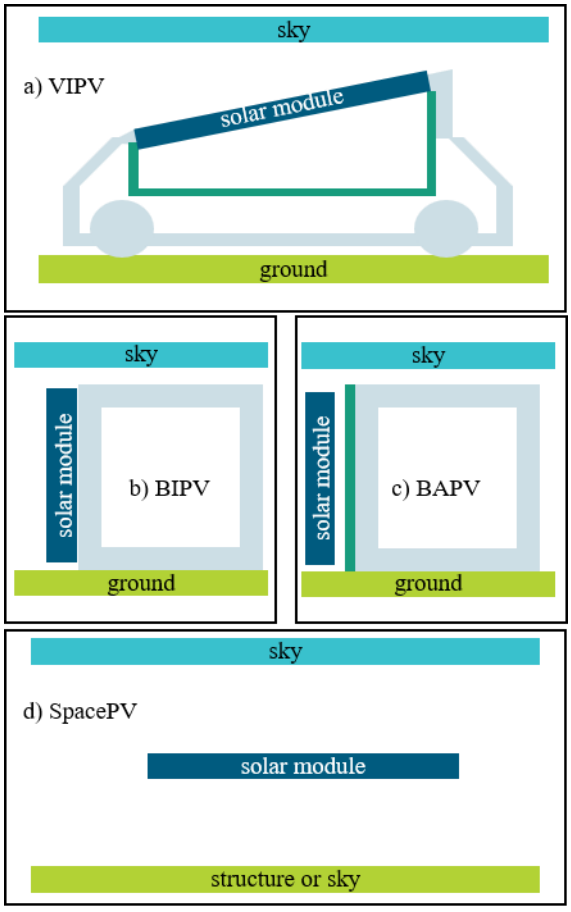

Figure 3: Schematic depiction of different integrated and mobile PV applications.

The colors in Figure 3 indicate how the changes of the model used for the free-standing module are transferred to calculate integrated or mobile applications (see Figure 2).

Table 1 gives a qualitative description of the changes necessary in the model for free-standing PV and for each application and their depiction in Figure 3.

Table 1: Qualitative changes of the thermal model for each application type

Free-Standing PV / NMOT	– Ambient temperature front ≠ ambient temperature rear – Wind speed front ≠ wind speed rear – Ground emissivity front ≠ ground emissivity rear – Ground temperature front ≠ ground temperature rear – Sky temperature front ≠ sky temperature rear – Sky emissivity front ≠ sky emissivity rear
VIPV	– Car air temperature ≠ ambient temperature – Car container temperature = car air temperature – Wind speed inside = 0 m/s – Emissivity of car interior ≠ ground emissivity – Solar module replaces car roof (no added layer behind the module, roofing structure may be added as module layer) – Tilted module possible
BIPV	– Building air temperature ≠ ambient temperature – Building wall temperature = building air temperature – Wind speed inside the building = 0 m/s – Emissivity of building interior ≠ ground emissivity – Additional layer is added to the module (the wall), full contact of the module to the wall is assumed – Heat exchange with the building interior
BAPV	– Module rear sees no sky – Building properties replace sky properties for rear side – Ground emissivity and sky emissivity rear are replaced by building emissivity – Ground temperature and sky temperature rear are replaced by building temperature – Ambient temperature front ≠ ambient temperature rear – Wind speed front ≠ wind speed rear
SpacePV	– No Convection – No direct heat transfer to environment – Different emissivity for sky and a rear structure possible – Ground emissivity rear = sky emissivity rear – Ground temperature rear = sky temperature rear

With the implementation of these changes other applications are possible. To specifically allow for the assessment of BIPV the wall as an additional element is added and heat exchange with the interior of the building is included. The separation of BIPV and BAPV is necessary since in BAPV the module rear side may see wind and convection and the building wall is not directly connected to the module.

Table 2: Specific parameters for each application type

Free-Standing PV	– 1000 W/m² AM1.5 perpendicular direct front irradiance, – 0 W/m² rear irradiance – 25 °C ambient and ground temperature (front and rear side) – 45° module inclination – v_{wind} = 1 m/s (front and rear side) – ε_{ground} = 0.9 (front and rear side)
NMOT	– 800 W/m² AM1.5 perpendicular direct front irradiance, – 0 W/m² rear irradiance – 20 °C ambient and ground temperature (front and rear side) – 45° module inclination – v_{wind} = 1 m/s (front and rear side) – ε_{ground} = 0.9 (front and rear side)
VIPV	– $t_{ambient}$ = 25 °C, $t_{interior}$ = 20 °C – $v_{wind,\ front}$ = 13.9 m/s (50 km/h), – $v_{wind,\ interior}$ = 0 m/s – No additional layer considered (module = car roof) – 0° module inclination (horizontal module mounting)
BIPV	– $t_{ambient}$ = 25 °C, $t_{interior}$ = 20 °C – $v_{wind,\ outside}$ = 1 m/s, $v_{wind,\ interior}$ = 0 m/s – 90° module inclination (vertical module mounting) – KfW40 wall: U-value = 0.14 W/m²K: thermal conductivity = 0.07 W/mK, thickness = 0.48 m
BAPV	– 25 °C ambient, ground and building temperature – 1 m/s wind on module front, 0 m/s on rear side – 90° module inclination (vertical module mounting)
SpacePV	– No mounting structure: module is free floating in space – Irradiance front = 1367 W/m², AM_0 – $T_{ambient}$ = -270.4 °C – Emissivity of space = 1

Calculations for free-standing PV and Nominal Module Operating Temperature (NMOT) Conditions both use the thermal model for the free-standing PV module.

The extended thermal model is implemented into a Cell-to-Module (CTM) loss channel analysis software ("SmartCalc.Module") and the impact of module application on module temperature is analyzed [14].

Cell-to-Module (CTM) analysis is a bottom-up multi-physics loss-channel analysis that quantifies gains and losses from solar cell to module output and groups gains and losses into loss channels. The single loss channels may represent relevant geometrical (i.e. cell overlap) or physical effects (i.e. resistive losses) or module components (i.e. the junction box) [15–17]. CTM analysis has become an accepted method to analyze module concepts and the losses occurring from integration of solar cells into modules under Standard Testing Conditions (STC), the impact of operation conditions on module power output (non-STC) as well as distinctive characteristics of modules regarding performance or degradation [9,18]. The analysis of non-STC conditions requires thermal models to allow for the calculation of interactions between operation conditions, module design and material properties, as well as loss mechanisms [1–7].

We apply the thermal model on a conventional glass-glass TOPCon module (120 × 26.2% G12R TOPCon half cells, 18 round wires, 2x 1.8 mm glass) to demonstrate the effect of the application on the module temperature. We are aware that specific changes to the module would be necessary or at least recommended for each application, but to highlight the impact of the thermal model on power output, the module is left unchanged.

It may be noted that for each of the applications not only the PV module is the same but also all irradiance is perpendicular and direct. Especially for vertical integration this is likely unrealistic but any additional introduction of tilted angles of irradiance would further complicate the comparison of the thermal effects. The models are capable of analyzing non-perpendicular and diffuse irradiance.

III. RESULTS

We calculated the module efficiency at Standard Testing Conditions (STC) to be 22.7% (Figure 4).

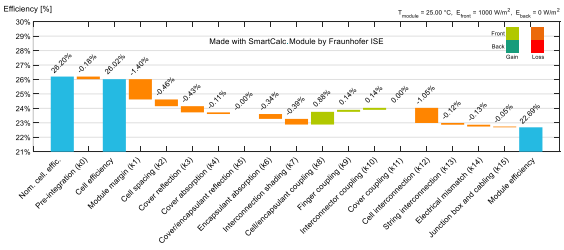

Figure 4: Cell-to-Module (CTM) analysis of the module at Standard Testing Conditions

The same module at the free-standing non-STC conditions unsurprisingly has a lower output efficiency of 19.5%. Since spectrum and irradiance intensity are unchanged, only thermal losses occur which account for 3.2%$_{abs}$ (Figure 5). The module temperature increases to 59.6 °C.

The solar cell temperature is especially low for the VIPV application. The strong headwind (50 km/h) leads to an effective cooling. Front convection is the dominant heat dissipation mechanism in this case (Figure 6). Energy dissipation to the vehicle interior is small (29 W/m²) in this scenario.

Comparing BIPV and BAPV, we find BAPV to have a higher cell temperature (+2.4 K). Heat conduction through the wall effectively dissipates energy and lowers the module temperature for BIPV. The airgap between the BAPV module and the wall and the low convection (1m/s wind speed behind the BAPV module) are effective thermal barriers in our analysis.

For SpacePV a change in intensity (1000 W/m² to 1367 W/m²) and spectrum (AM1.5 to AM0) occurs. Several optical effects (i.e. UV absorption in the encapsulant), the spectral response of the solar cell, and higher resistive losses within the module lower the module output compared to the irradiant energy. Therefore, an additional category of losses is shown in Figure 5 for SpacePV. The new category contains power changes resulting from changes in spectrum, angular distribution and intensity of the incoming light compared to

1000 W/m² direct perpendicular irradiance with an AM1.5 spectrum. For NMOT only the intensity of the irradiant light changes (800 W/m²). The spectral and intensity loss channel therefore only contains changes from intensity here. The change in module efficiency is positive as power losses within the module decrease even more than the intensity of the incoming light (i.e. quadratic reduction of ohmic losses in cell interconnector ribbons).

The thermal losses in SpacePV are comparable to terrestrial applications (-2.4%$_{abs}$) and the module temperature is also in a moderate level (51.6 °C – under irradiance, static calculation). Since more energy is entering the module, heat dissipation is increased for SpacePV but only radiative heat loss as well module power output occurs (Figure 6).

While only part of the energy balance of the module but not of the heat exchange, module reflection needs to be considered. It accounts for 15 W/m² all operating conditions except for SpacePV (31 W/m²) and NMOT (10 W/m²). Reflected light does not cause heat that needs to be dissipated but also does not generate electrical power. The heat generation is mostly concentrated on the solar cell, as the solar cell is designed to be an excellent absorber of light (Figure 8).

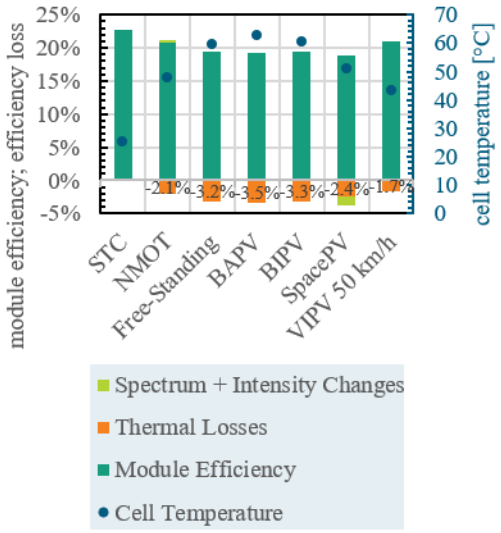

Figure 5: Module output efficiency, loss channels and cell temperature of the analyzed module applications

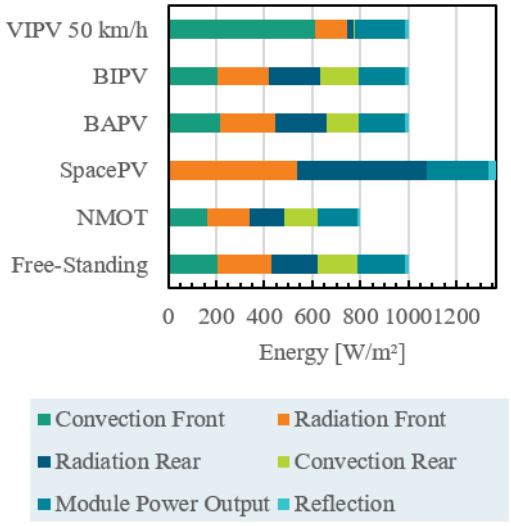

Figure 6: Temperature dissipation mechanisms for each application type

The analysis shows the importance of both module surfaces for heat dissipation. Only for VIPV a largely extended heat dissipation through the module front is observed. Heat dissipation through the module's rear side only accounts for 28 W/m² which is also visible in the module rear surface temperature (43.0 °C) which is elevated compared to the front surface temperature (40.8 °C) (Figure 7).

Also, the importance of module power output as a heat sink is evident. Lower module temperatures can therefore be expected as module efficiency increases.

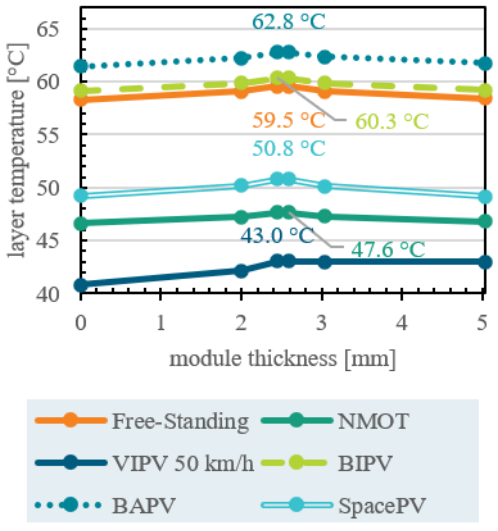

Figure 7: Temperature profile of the modules under the analyzed conditions. Total module thickness is 5.04 mm, each glass is 2.0 mm, and the encapsulant films are 0.45 mm.

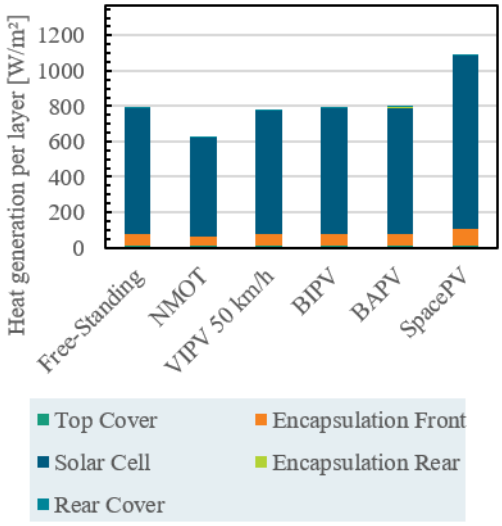

Figure 8: Heat sources per layer

As mentioned above and published by [19], the vehicle speed has a significant impact on module power output and temperature. We therefore extended the simulations for different vehicle speeds ranging from 10 km/h to 50 km/h.

We find the module temperature to decrease with higher vehicle speed (Figure 9) as the front convection increases (Figure 10). With increasing speed, the thermal losses decrease and module power output increases.

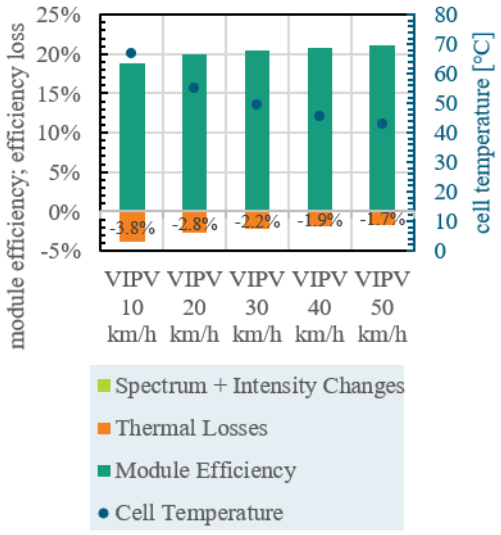

Figure 9: VIPV module power output and cell temperature

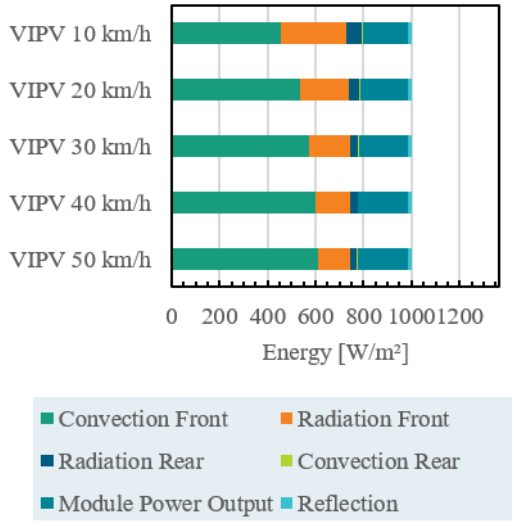

Figure 10: VIPV module heat dissipation

Figure 10 shows an increase of irradiant heat dissipation for the module rear side for lower vehicle speed which might affect passengers and their comfort.

IV. DISCUSSION

The presented model is based on established energy-balance equations describing conductive, convective, and radiative heat transfer. These governing equations are widely used in engineering applications and form the basis of numerous validated thermal models. In particular, one-dimensional, layer-resolved thermal models for PV modules have been extensively reported in the literature, with several studies demonstrating their applicability through comparison with experimental data [1–7].

Accordingly, this work builds on an established physical modelling framework and does not aim to revalidate the underlying heat-transfer equations or the general approach of one-dimensional PV module thermal modelling. The extensions introduced in this study primarily concern the representation of application-specific boundary conditions, including separate front- and rear-side environments, building interfaces, vehicle interiors, and space environments.

However, no dedicated experimental validation of these newly introduced application-specific model extensions has been performed within this work. Therefore, the presented results should be interpreted as comparative model predictions. Their quantitative accuracy depends on the appropriateness of the selected boundary conditions, material parameters, and assumptions for each application.

Experimental validation under representative VIPV, BIPV, BAPV, and SpacePV operating conditions remains subject to future work.

To nonetheless provide orientation about the presented extensions of the original model [6], we calculate the nominal module operating temperature (NMOT) and compare it to several empirical thermal models [20–29].

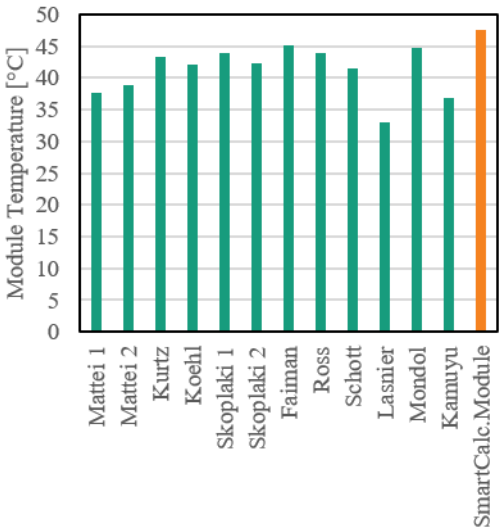

Figure 11: Comparison of our thermal model and existing other empirical thermal models for Normal Module Operating Temperature (NMOT, 800 W/m², 25 °C, 1 m/s)

We find the NMOT calculated by our model to be higher than the temperature of the other models (+6.5 K on average). Technical module datasheets state NMOT in the range of 43 °C which is 4.6 K lower than our calculation.

The difference is significant, but some aspects need to be considered in the interpretation.

The presented model currently does not consider inactive module areas (i.e. edge spacing or frame) due to its one-dimensional modelling approach which would act as additional heat sinks. Furthermore it does not consider edge effects (i.e. stronger wind cooling along the edges), and its heat transfer coefficients are not empirically finetuned to match certain outdoor conditions but taken only from literature [6].

Future improvements considering the named shortcomings might therefore improve the model and close the gap between other models and observations.

It might also be noted that while the presented model has an offset compared to other models, a comparison between two module designs may still provide useful insights and that the other models cannot be easily applied to other module stacks, technologies, and materials without adjustments as those are empirical models.

V. IV. SUMMARY

This paper extends an analytical one-dimensional thermal model for PV modules to account for different environmental conditions at the module front and rear sides. The extension enables simulations of free-standing PV, vehicle-integrated PV (VIPV), building-integrated PV (BIPV), building-attached PV (BAPV), and space PV (SpacePV).

The model was integrated into a Cell-to-Module (CTM) loss-channel analysis and applied to a conventional glass-glass TOPCon module. The results show that the application environment strongly affects module temperature, heat dissipation mechanisms, and electrical output.

VIPV showed particularly effective cooling because of high vehicle-induced airflow, with front-side convection becoming the dominant heat-loss mechanism. BIPV modules operated cooler than BAPV modules because heat conduction through the building wall provided an additional heat path. In space, where convection is absent, heat rejection occurred exclusively through radiation and electrical power generation.

Overall, the proposed extensions substantially broaden the applicability of analytical PV thermal models for integrated and mobile PV systems. However, the new model extensions have not yet been experimentally validated. A comparison of our model to empirical models shows differences of around 6.5 K.

References

[1] A.K. Abdulrazzaq, B. Plesz, G. Bognár, A Novel Method for Thermal Modelling of Photovoltaic Modules/Cells under Varying Environmental Conditions, Energies 13 (2020) 3318. https://doi.org/10.3390/en13133318.

[2] W. Gu, T. Ma, L. Shen, M. Li, Y. Zhang, W. Zhang, Coupled electrical-thermal modelling of photovoltaic modules under dynamic conditions, Energy 188 (2019) 116043. https://doi.org/10.1016/j.energy.2019.116043.

[3] H. Hanifi, S. Regondi, B. Jaeckel, J. Schneider, 2020. Determination of electrical characteristics and temperature of PV modules by means of a coupled electrical-thermal model. Journal of Renewable and Sustainable Energy 12, 023501. https://doi.org/10.1063/5.0001599.

[4] Z.H. Lu, Q. Yao, Energy analysis of silicon solar cell modules based on an optical model for arbitrary layers, Solar Energy 81 (2007) 636–647. https://doi.org/10.1016/j.solener.2006.08.014.

[5] T. Ma, Z. Guo, L. Shen, X. Liu, Z. Chen, Y. Zhou, X. Zhang, Performance modelling of photovoltaic modules under actual operating conditions considering loss mechanism and energy distribution, Applied Energy 298 (2021) 117205. https://doi.org/10.1016/j.apenergy.2021.117205.

[6] M. Mittag, L. Vogt, C. Herzog, A. Pfreundt, J. Shahid, D.H. Neuhaus, H. Wirth, Thermal Modelling of Photovoltaic Modules in Operation and Production. 9 pages / 36th European Photovoltaic Solar Energy Conference and Exhibition; 892-900 / 36th European Photovoltaic Solar Energy Conference and Exhibition; 892-900 (2019). https://doi.org/10.4229/EUPVSEC20192019-4CO.2.4.

[7] G. Notton, C. Cristofari, M. Mattei, P. Poggi, Modelling of a double-glass photovoltaic module using finite differences, Applied Thermal Engineering 25 (2005) 2854–2877. https://doi.org/10.1016/j.applthermaleng.2005.02.008.

[8] A. Thomson, M. Ernst, I. Haedrich, J. Qian, Impact of PV module configuration on energy yield under realistic conditions, Opt Quant Electron 49 (2017). https://doi.org/10.1007/s11082-017-0903-0.

[9] A. Pfreundt, J. Shahid, M. Mittag, Cell-to-module Analysis beyond Standard Test Conditions, in: 2020 47th IEEE Photovoltaic Specialists Conference (PVSC), Calgary, AB, Canada, IEEE, 2020, pp. 921–926.

[10] H. Hanifi, C. Pfau, M. Turek, J. Schneider, A practical optical and electrical model to estimate the power losses and quantification of different

heat sources in silicon based PV modules, Renewable Energy 127 (2018) 602–612. https://doi.org/10.1016/j.renene.2018.04.060.

[11] H. Yousuf, M.A. Zahid, M.Q. Khokhar, J. Park, M. Ju, D. Lim, Y. Kim, E.-C. Cho, J. Yi, Cell-to-Module Simulation Analysis for Optimizing the Efficiency and Power of the Photovoltaic Module, Energies 15 (2022) 1176. https://doi.org/10.3390/en15031176.

[12] M.H. Saw, Y.S. Khoo, J.P. Singh, Y. Wang, Cell-to-module optical loss/gain analysis for various photovoltaic module materials through systematic characterization, Jpn. J. Appl. Phys. 56 (2017) 08MD03. https://doi.org/10.7567/JJAP.56.08MD03.

[13] M. Mittag, A. Pfreundt, J. Shahid, N. Wöhrle, D.H. Neuhaus, Techno-Economic Analysis of Half-Cell Modules - The Impact of Half-Cells on Module Power and Costs. 8 pages / 36th European Photovoltaic Solar Energy Conference and Exhibition; 1032-1039 / 36th European Photovoltaic Solar Energy Conference and Exhibition; 1032-1039 (2019). https://doi.org/10.4229/EUPVSEC20192019-4AV.1.20.

[14] Fraunhofer ISE, SmartCalc.Module, Freiburg, 2026.

[15] I. Haedrich, U. Eitner, M. Wiese, H. Wirth, Unified methodology for determining CTM ratios: Systematic prediction of module power, Solar Energy Materials and Solar Cells 131 (2014) 14–23. https://doi.org/10.1016/j.solmat.2014.06.025.

[16] M. Mittag, C. Kutter, S. Hoffmann, P. Romer, A.J. Beinert, T. Zech, Electrical and Thermal Modeling of Junction Boxes. 6 pages / 33rd European Photovoltaic Solar Energy Conference and Exhibition; 1501-1506 (2017). https://doi.org/10.4229/EUPVSEC20172017-5DO.5.5.

[17] M. Mittag, T. Zech, M. Wiese, D. Blasi, M. Ebert, H. Wirth, Cell-to-Module (CTM) Analysis for Photovoltaic Modules with Shingled Solar Cells, in: 2017 IEEE 44th Photovoltaic Specialist Conference (PVSC), Washington, DC, USA, IEEE, 2017, pp. 1531–1536.

[18] A. Tummalieh, M. Mittag, C. Reichel, A. Protti, H. Neuhaus, Holistic Analysis for Mismatch Losses in Photovoltaic Modules: Assessing the Impact of Inhomogeneity from Operational Conditions and Degradation Mechanisms on Power and Yield, Progress in Photovoltaics 34 (2026) 39–59. https://doi.org/10.1002/pip.3865.

[19] L.E. Alanis, A. Velte-Schäfer, N. Jajoo, M.-A. Schüler, L.C. Rendler, D.H. Neuhaus, M. Heinrich, Thermal effect of VIPV modules in refrigerated trucks, Solar Energy Materials and Solar Cells 275 (2024) 113000. https://doi.org/10.1016/j.solmat.2024.113000.

[20] W. Charles Lawrence Kamuyu, J. Lim, C. Won, H. Ahn, Prediction Model of Photovoltaic Module Temperature for Power Performance of Floating PVs, Energies 11 (2018) 447. https://doi.org/10.3390/en11020447.

[21] J.D. Mondol, Y.G. Yohanis, B. Norton, Comparison of measured and predicted long term performance of grid a connected photovoltaic system, Energy Conversion and Management 48 (2007) 1065–1080. https://doi.org/10.1016/j.enconman.2006.10.021.

[22] F. Lasnier, Photovoltaic engineering handbook, Adam Higler, Bristol, 1990.

[23] T. Schott, Operating Temperatures of PV Modules, in: 6th EC Photovoltaic Solar Energy Conference 1985.

[24] Ross, R. G., Jr., Interface design considerations for terrestrial solar cell modules, in: 12th Photovoltaic Specialists Conference 1976, pp. 801–806.

[25] M. Mattei, G. Notton, C. Cristofari, M. Muselli, P. Poggi, Calculation of the polycrystalline PV module temperature using a simple method of energy balance, Renewable Energy 31 (2006) 553–567. https://doi.org/10.1016/J.RENENE.2005.03.010.

[26] M. Koehl, M. Heck, S. Wiesmeier, J. Wirth, Modeling of the nominal operating cell temperature based on outdoor weathering, Solar Energy Materials and Solar Cells 95 (2011) 1638–1646. https://doi.org/10.1016/j.solmat.2011.01.020.

[27] S. Kurtz, K. Whitfield, G. TamizhMani, M. Koehl, D. Miller, J. Joyce, J. Wohlgemuth, N. Bosco, M. Kempe, T. Zgonena, Evaluation of high-temperature exposure of photovoltaic modules, Progress in Photovoltaics 19 (2011) 954–965. https://doi.org/10.1002/pip.1103.

[28] D. Faiman, Assessing the outdoor operating temperature of photovoltaic modules, Progress in Photovoltaics 16 (2008) 307–315. https://doi.org/10.1002/pip.813.

[29] E. Skoplaki, J.A. Palyvos, Operating temperature of photovoltaic modules: A survey of pertinent correlations, Renewable Energy 34 (2009) 23–29. https://doi.org/10.1016/j.renene.2008.04.009.